Journal of Visualized Experiments

An Optimized O9-1/hydrogel System for Studying Mechanical Signals in Neural Crest Cells

--Manuscript Draft--

Article Type:	Invited Results Article - JoVE Produced Video
Manuscript Number:	JoVE62693R2
Full Title:	An Optimized O9-1/hydrogel System for Studying Mechanical Signals in Neural Crest Cells
Corresponding Author:	Jun Wang, Ph.D. University of Texas McGovern Medical School: The University of Texas Health Science Center at Houston John P and Katherine G McGovern Medical School Houston, Texas UNITED STATES
Corresponding Author's Institution:	University of Texas McGovern Medical School: The University of Texas Health Science Center at Houston John P and Katherine G McGovern Medical School
Corresponding Author E-Mail:	Jun.Wang@uth.tmc.edu
Order of Authors:	Tram P Le
	Xiaolei Zhao
	Shannon Erhardt
	Jianhua Gu
	Huie Wang
	Tina Findley
	Jun Wang
Additional Information:	
Question	**Response**
Please indicate whether this article will be Standard Access or Open Access.	Standard Access (US$2,400)
Please specify the section of the submitted manuscript.	Developmental Biology
Please indicate the **city, state/province, and country** where this article will be **filmed**. Please do not use abbreviations.	Houston, TX USA
Please confirm that you have read and agree to the terms and conditions of the author license agreement that applies below:	I agree to the Author License Agreement
Please provide any comments to the journal here.	
Please indicate whether this article will be Standard Access or Open Access.	Standard Access ($1400)
Please confirm that you have read and agree to the terms and conditions of the video release that applies below:	I agree to the Video Release

TITLE:

An Optimized O9-1/hydrogel System for Studying Mechanical Signals in Neural Crest Cells

AUTHORS AND AFFILIATIONS:

Tram P. Le[1#], Xiaolei Zhao[1#], Shannon Erhardt[1], Jianhua Gu[2], Huie Wang[2], Tina O. Findley[1], Jun Wang[1]

[1]Department of Pediatrics, McGovern Medical School, The University of Texas Health Science Center at Houston, Houston, Texas, USA

[2]SEM AFM Core in the Houston Methodist Hospital Research Institute, Houston, Texas, USA

[#]Contributed equally

Email addresses of co-authors:

Tram P. Le	(tram.p.le@uth.tmc.edu)
Xiaolei Zhao	(xiaolei.zhao@uth.tmc.edu)
Shannon Erhardt	(shannon.erhardt@uth.tmc.edu)
Jianhua Gu	(jgu@houstonmethodist.org)
Huie Wang	(hwang4@houstonmethodist.org)
Tina O. Findley	(tina.o.findley@uth.tmc.edu)

Corresponding author:

Jun Wang (jun.wang@uth.tmc.edu)

KEYWORDS:

neural crest cells, mechanical signals, O9-1 cells, atomic force microscopy

SUMMARY:

Detailed step-by-step protocols are described here for studying mechanical signals *in vitro* using multipotent O9-1 neural crest cells and polyacrylamide hydrogels of varying stiffness.

ABSTRACT:

Neural crest cells (NCCs) are vertebrate embryonic multipotent cells that can migrate and differentiate into a wide array of cell types that give rise to various organs and tissues. Tissue stiffness produces mechanical force, a physical cue that plays a critical role in NCC differentiation; however, the mechanism remains unclear. The method described here provides detailed information for the optimized generation of polyacrylamide hydrogels of varying stiffness, the accurate measurement of such stiffness, and the evaluation of the impact of mechanical signals in O9-1 cells, a neural crest cell line that mimics *in vivo* NCCs.

Hydrogel stiffness was measured using atomic force microscopy (AFM) and indicated different stiffness levels accordingly. O9-1 NCCs cultured on hydrogels of varying stiffness showed different cell morphology and gene expression of stress fibers, which indicated varying biological effects caused by mechanical signal changes. Moreover, this established that varying the

hydrogel stiffness resulted in an efficient *in vitro* system to manipulate mechanical signaling by altering gel stiffness and analyze the molecular and genetic regulation in NCCs. O9-1 NCCs can differentiate into a wide range of cell types under the influence of the corresponding differentiation media, and it is convenient to manipulate chemical signals *in vitro*. Therefore, this *in vitro* system is a powerful tool to study the role of mechanical signaling in NCCs and its interaction with chemical signals, which will help researchers better understand the molecular and genetic mechanisms of neural crest development and diseases.

INTRODUCTION:

Neural crest cells (NCCs) are a group of stem cells during vertebrate embryogenesis with a remarkable ability to migrate and contribute to the development of various organs and tissues. NCCs can differentiate into different cell types, including sensory neurons, cartilage, bone, melanocytes, and smooth muscle cells, depending on the location of axial origin and the local environmental guidance of the NCC[1-2]. With the ability to differentiate into a wide array of cell types, genetic abnormalities that cause dysregulation at any stage of neural crest (NC) development can lead to numerous congenital diseases[2]. For instance, perturbations during the formation, migration, and development of NCCs lead to developmental disorders known collectively as neurocristopathies[1,3]. These diseases range from craniofacial defects due to failure in NCC formation, such as Treacher Collins syndrome, to the development of various cancers due to NCC metastatic migratory ability, as seen in melanoma[3,4,5,6]. Over the last few decades, researchers have made remarkable discoveries about the roles and mechanisms of NCCs in development and diseases, with the majority of findings being focused on chemical signals[7,8]. More recently, mechanical signals have been indicated to play a critical but poorly understood role in NCC development[9,10].

The environmental cues of NCCs play a critical role during their development, including the regulation of NCC differentiation into various cell types. Environmental cues, e.g., physical cues, influence pivotal behaviors and cellular responses, such as functional diversification. Mechanotransduction allows cells to sense and respond to those cues to maintain various biological processes[2]. NCCs are surrounded by neighboring cells and different substrates, such as the extracellular matrix (ECM), which can give rise to mechanical stimuli to maintain homeostasis and adapt to the changes through fate determination, proliferation, and apoptosis[11]. Mechanotransduction begins at the plasma membrane where the sensory component of mechanical extracellular stimuli occurs, resulting in the intracellular regulation of the cell[12]. Integrins, focal adhesions, and junctions of the plasma membrane relay mechanical signals, such as shearing forces, stress, and the stiffness of surrounding substrates, into chemical signals to produce cellular responses[12]. The relaying of chemical signals from the plasma membrane to the final cellular regulation is carried out via different signaling pathways to finalize vital processes for the organism, such as differentiation.

Several studies have suggested that mechanical signaling from substrate stiffness plays a role in cell differentiation[13,14]. For instance, previous studies have shown that mesenchymal stem cells (MSCs) grown on soft substrates with a stiffness similar to that of brain tissue (in the range of 0.1–1.0 kPa) resulted in neuronal cell differentiation[15,16]. However, more MSCs differentiate into

myocyte-like cells when grown on 8–17 kPa substrates mimicking the stiffness of muscle, while osteoblast-like differentiation was observed when MSCs were cultured on stiff substrates (25–40 kPa)[15,16]. The significance of mechanotransduction is highlighted by the irregularities and abnormalities in the mechanical signaling pathway that potentially lead to severe developmental defects and diseases, including cancer, cardiovascular diseases, and osteoporosis[17,18,19]. In cancers, normal breast tissue is soft, and the risk of breast cancer increases in stiff and dense breast tissue, an environment that is more akin to breast tumors[15]. With this knowledge, the effects of mechanical signaling on NCC development can be studied through simple manipulation of substrate stiffness through an *in vitro* system, providing further advantages and possibilities in understanding the fundamentals of NC-related disease progression and etiology.

To study the impact of mechanical signals in NCCs, we established an efficient *in vitro* system for NCCs based on the optimization of previously published methods and evaluation of the responses of NCCs to different mechanical signal[20,21]. A detailed protocol was provided for varying hydrogel stiffness preparation and evaluation of the impact of mechanical signaling in NCCs. To achieve this, O9-1 NCCs are utilized as the neural crest (NC) model to study the effects and changes in response to stiff versus soft hydrogels. O9-1 NCCs are a stable NC cell line isolated from mouse embryo (E) at day 8.5. O9-1 NCCs mimic NCCs *in vivo* because they can differentiate into various NC-derived cell types in defined differentiation media[22]. To study the mechanical signaling of NCCs, a matrix substrate was fabricated with tunable elasticity from varying concentrations of acrylamide and bis-acrylamide solutions to achieve the desired stiffness, correlating to the biological substrate stiffness[20,21,23]. To optimize the conditions of matrix substrate for NCCs, specifically O9-1 cells, modifications were made from the previously published protocol[20]. One change made in this protocol was to incubate hydrogels in collagen I, diluted in 0.2% acetic acid instead of 50 mM HEPES, at 37 °C overnight. The low pH of acetic acid leads to a homogeneous distribution and higher collagen I incorporation, thus allowing for a more uniform attachment of the ECM protein[24]. In addition, a combination of horse serum and FBS was used at the concentrations of 10% and 5% in PBS, respectively, before storing the hydrogels in the incubator. Horse serum was used as an additional supplement to FBS due to its ability to promote cell proliferation and differentiation at the concentration of 10%[25].

With this method, a biological environment was mimicked by the ECM protein coating (e.g., Collagen I) to create an accurate *in vitro* environment for NCCs to grow and survive[20,21]. The stiffness of the prepared hydrogels was quantitatively analyzed via atomic force microscopy (AFM), a well-known technique to depict the elastic modulus[26]. To study the effect of different stiffness levels on NCCs, wild-type O9-1 cells were cultured and prepared on hydrogels for immunofluorescence (IF) staining against F-actin to show the differences in cell adhesion and morphologies in response to changes in substrate stiffness. Utilizing this *in vitro* system, researchers will be able to study the roles of mechanical signaling in NCCs and its interaction with other chemical signals to gain a deeper understanding of the relationship between NCCs and mechanical signaling.

PROTOCOL:

1. Hydrogel preparation

NOTE: All steps must be performed in a cell culture hood that has been disinfected with ethanol and UV-sterilized before use to maintain sterility. Tools, such as tweezers and pipettes, must be sprayed with ethanol. Buffer solutions must also be sterile-filtered.

1.1. Preparation of aminosilane-coated glass coverslips

1.1.1. Place the desired number of glass coverslips onto a piece of laboratory wipe.

NOTE: Prepare an additional 3–4 coverslips to ensure sufficient backup supplies as they break easily. Different materials of glass coverslips will yield different compatibility of cell seeding and attachment. It is better to determine which type suits the experiment best before starting the experiments (see the **Table of Materials)**.

1.1.2. Use an alcohol burner or Bunsen burner to sterilize each coverslip by passing it back and forth through the flame (30 s for protein assay experiments). Place each glass coverslip on a laboratory wipe to cool down.

1.1.3. Once the glass coverslips are cooled down, transfer them onto a Petri dish lined with parafilm to prevent slippage.

NOTE: If the coverslips are not cool enough, the residual heat will melt the parafilm onto the slips, rendering them unusable.

1.1.4. Cover the coverslips with approximately 200 µL and 800 µL of 0.1 M NaOH for a 12 mm and a 25 mm coverslip, respectively, and let them sit for 5 min. Then, aspirate the 0.1 M NaOH and allow the coverslips to air-dry for another 5 min to form an even film.

1.1.5. Once the coverslips are dried, pipette approximately 80 µL and 150 µL of 3-aminopropyl triethoxysilane (APTS) for 12 mm and 25 mm coverslips, respectively. Be careful to avoid spilling the solution onto the parafilm. Allow the solution to sit for 5 min.

1.1.6. Aspirate as much excess APTS as possible and allow the residual APTS to dry for 5 min. Rinse the coverslips well by submerging them in sterile, deionized (DI) H_2O three times for 5 min each time.

NOTE: If the glass coverslips are not rinsed well, the residual APTS causes unwanted reactions with glutaraldehyde, causing a white precipitate to form and resulting in unusable coverslips.

1.1.7. Move the coverslips to a new Petri dish with the reactive side facing up. Add enough 0.5% glutaraldehyde to the Petri dish to cover the coverslips entirely and allow the coverslips to sit for 30 min.

1.1.8. Aspirate the 0.5% glutaraldehyde and rinse the coverslips again in DI H_2O one time for 3 min. Set the coverslips reactive side up on a laboratory wipe or a clean Petri dish to air-dry completely before using.

NOTE: The protocol can be paused here; coverslips must be placed in sterile DI H_2O until use.

1.2. Preparation of siliconized coverslips

1.2.1. Place the same number of coverslips as the aminosilane-coated coverslips (step 1.1.1) in a Petri dish lined with parafilm.

1.2.2. Pipette 40 µL or 150 µL for 12 mm and 25 mm coverslips, respectively, of dichloromethylsilane (DCMS) to one side of the coverslip and allow the solution to sit for 5 min.

1.2.3. Aspirate any remaining solution from the coverslip, wash in sterile DI H_2O once for 1 min, and place the reactive coverslips face up on a laboratory wipe to air-dry completely before moving onto the next step.

1.3. Preparing hydrogels

1.3.1. Mix acrylamide, bis-acrylamide, and DI H_2O in a 1.5 mL centrifuge tube to prepare 500 µL of solutions with varying stiffnesses (see **Table 1**). Vortex the solution for 30 s to mix it thoroughly.

1.3.2. Working swiftly, add the 10% ammonium persulfate solution (APS) and tetramethylethylenediamine (TEMED) to the tube and vortex the solutions again to mix the solutions.

NOTE: Prepare fresh 10% APS and leave it on ice or freeze into single-use aliquots due to its sensitive freeze/thaw cycle.

1.3.3. Pipette approximately 33 µL or 100 µL of the solution onto the dried 12 mm or 25 mm aminosilane-coated coverslips (section 1.1), respectively.

1.3.4. Using curved tweezers, immediately place the DCMS-treated coverslip on top of the gel solution with the treated side touching the gel solution, thus sandwiching the gel solution between the DCMS-treated coverslip and aminosilane-coated coverslip.

1.3.5. Allow the gel solution to polymerize for 5–15 min, while actively monitoring for gel polymerization of the leftover solution in the tube.

1.3.6. Once the gel is polymerized, separate the DCMS-treated coverslip with curved tweezers or a razor blade, leaving the gel attached to the original aminosilane-coated coverslip.

1.3.7. Immediately place the coverslip with the attached hydrogel in a predetermined 4-well/24-well or 6-well plate covered with 500 µL or 2 mL of sterile phosphate-buffered saline (PBS) or DI H_2O for 12 mm and 25 mm coverslips, respectively, to prevent the gel from drying out.

1.3.8. Repeat steps 1.3.4–1.3.7 for all coverslips.

1.3.9. Submerge the hydrogels in sterile PBS or DI H_2O for 30 min to remove excess acrylamide solution. Store the hydrogels in sterile PBS or DI H_2O at 4 °C for a procedural stop here.

1.3.10. In a dark room, prepare the sulfosuccinimidyl 6-(4'-azido-2'-nitrophenylamino) hexanoate (sulfo-SANPAH) mixture by mixing 2.5 mL of 50 mM 2-[4-(2-hydroxyethyl) piperazin-1-yl] ethanesulfonic acid (HEPES) (pH=8.5) with 25 µL of the 50 µg/mL sulfo-SANPAH in a conical tube, wrapped in aluminum foil to protect from light. Use a pipette to mix the solution well before using.

NOTE: A volume of 2.5 mL of sulfo-SANPAH solution is enough for approximately twenty-five 12 mm hydrogels or five 25 mm hydrogels.

1.3.11. Aspirate PBS or DI H_2O from the well plate. Add approximately 100 µL or 500 µL for 12 mm and 25 mm coverslips, respectively, of sulfo-SANPAH solution (step 1.3.10) to cover the gel. Ensure the solution covers the gel entirely.

NOTE: Adjust the vacuum suction strength to prevent the strong force from ripping or disturbing the hydrogels.

1.3.12. Place the gels with the solution under a 15 W, 365 nm ultraviolet (UV) light for 10 min, uncovered to minimize any interference of the UV light reacting with the sulfo-SANPAH.

1.3.13. Aspirate the excess sulfo-SANPAH by tilting the plate to collect as much of the solution as possible. Wash the gel with 50 mM HEPES two to three times.

1.3.14. Add 500 µL or 2 mL for 12 mm and 25 mm gels, respectively, of 50 mg/mL collagen I diluted in 0.2% acetic acid to each well containing the hydrogel. Allow the gels to incubate overnight in a 37 °C, 5% CO_2 incubator.

NOTE: Dilute collagen I in 0.2% acetic acid instead of 50 mM HEPES to promote homogenous distribution and attachment of collagen I.

1.3.15. Aspirate the collagen I and wash the gels with sterile PBS three times to remove excess collagen I for 5 min each wash. Incubate the hydrogels in PBS with 10% horse serum, 5% fetal bovine serum (FBS) for 2 h in the 37 °C, 5% CO_2 incubator.

NOTE: The addition of 10% horse serum promotes higher proliferation compared to only using FBS as done in the previous publication.

1.3.16. Aspirate the medium. Add 500 mL of sterile-filtered Dulbecco's Modified Eagle Medium (DMEM) with 10% FBS and 1% penicillin-streptomycin (P/S) to each well. Store the gels in the 37 °C, 5% CO_2 incubator until ready for cell culture.

1.3.17. Once ready, plate approximately 1.5×10^4 O9-1 cells/cm^2 in basal medium in the culture dishes. Incubate the cells for 2 days in an incubator at 37 °C, 5% CO_2. Check the cells for confluency to ensure that the cells are sufficiently attached to gels, and that the number of cells is enough before collecting for analysis.

NOTE: See the previously published protocol for the steps of recovery, passage, and collection of O9-1 cells[20].

1.3.18. Proceed to sections 2, 3, or 4 for further analysis of the hydrogels.

2. Quantitative analysis of stiffness via AFM

2.1. Start the AFM system computer, followed by the AFM controller (see the **Table of Materials**).

2.2. Mount the AFM cantilever on the AFM probe holder. Use a spherical cantilever with a 0.5 μm silica bead mounted at the end of the cantilever (cantilever with spherical bead).

NOTE: For stiffer hydrogels, such as 10 kPa, 20 kPa, and 40 kPa, a stiffer probe was used with the spring constant of 0.24 N/m. A softer probe was used for softer hydrogels, such as 0.5 kPa and 1 kPa, with a spring constant of 0.059 N/m.

2.3. Set the AFM software under **contact mode**.

2.4. Mount the silicon wafer onto the AFM sample stage to collect force curves by clicking on **Engage** for the cantilever to touch the silicon substrate, thus generating the force curves.

2.5. Use the force curves above (2.4) for calibration, click on **Calibrate** in the controlling software to obtain an average spring constant of the cantilever under thermal tune condition, and save the calibrated values in the controlling software.

2.6. Mount the samples by placing the coverslip with the attached hydrogel in a 60 mm Petri dish onto the AFM scanning stage. Add 3 mL of PBS into the dish before conducting measurements to prevent the gel from drying out.

2.7. Set the AFM to work in **contact mode** (fluid) to start measurement. Engage the spherical bead to continuously touch and lift from the gel sample.

2.8. Set the cantilever so that its deflection threshold remains at 10 nm. Keep the ramping size of the probe at 10 μm. Then, record the force curves as in step 2.4.

2.9. Acquire at least 20 force curves from at least 3 to 10 different spots across the surface of the hydrogel.

2.10. Calculate the average Young's modulus of ~20 force curves for each spot with AFM imaging and analysis software. Use extend ramp force curves and a linearized model (spherical). Calculate the average of all spots for each sample to yield the final stiffness.

NOTE: Young's modulus and related data (*i.e.,* standard deviations) are automatically saved as a spreadsheet.

2.11. Repeat steps 2.6–2.10 for all samples.

3. Molecular analysis of stiffness via immunofluorescence staining

3.1. Use tweezers to transport the coverslip to a new plate to minimize false signals from cells grown directly onto the plate. Wash the cells with 500 µL of sterile PBS three times to remove dead cells and any remaining culture medium.

3.2. Fix the cells using 500 µL of 4% paraformaldehyde (PFA) for 10 min at room temperature, undisturbed. Then, rewash the cells three times using 500 µL of PBS/well for 2 min each.

NOTE: Store at 4 °C for a procedural stop.

3.3. Treat the cells with 500 µL of 0.1% Triton X-100 for 15 min at room temperature. Then, wash the cells three times with 500 µL of PBS/well.

3.4. Block the cells with 250 µL of 10% donkey serum (diluted in PBS and 0.1% Tween 20) per well for 30 min at room temperature.

3.5. Incubate the cells with 250 µL of primary antibodies for 2 h at room temperature or overnight at 4 °C. Then, wash the cells three times with 500 µL of PBS/well for 5 min each.

NOTE: Anti-Vinculin (Vcl) (1:250) and anti-AP2 alpha (1:250) were used in this experiment and were diluted in 10% donkey serum.

3.6. Incubate the cells with corresponding secondary antibodies and/or phalloidin used for F-actin staining at a dilution of 1:400 in 250 µL of 10% donkey serum for 30 min at room temperature. Then, wash the cells three times with PBS for 5 min each.

NOTE: 568 nm Phalloidin can be co-incubated with 488 nm or 647 nm secondary antibodies or on its own.

3.7. Incubate the cells with 4',6-diamidino-2-phenylindole (DAPI, 1:1000 dilution) in 250 µL of PBS for 10 min followed by one last wash of PBS for 2 min.

3.8. Add 3–4 drops of mounting medium to each well. Store the samples at 4 °C to set for at least 2 h before imaging to ensure the mounting medium has set properly.

3.9. Capture images of at least 3 random frames per hydrogel sample with a fluorescence microscope, producing individual and merged channels.

4. Quantitative real-time PCR (RT-qPCR)

4.1. Transfer the hydrogels with the adherent cells for RNA collection to a new plate to minimize unwanted RNA from cells attached to the cell plate. Wash the cells with PBS three times to remove dead cells and culture medium.

4.2. Extract the total mRNA using an RNA extraction kit. Perform reverse-transcription of RNA to cDNA using a reverse transcription supermix following the manufacturer's instructions.

4.3. Perform RT-qPCR with primers for *Vcl* as the stiffness marker of choice and analyze using the $2^{-\Delta\Delta CT}$ method.

NOTE: Primer sequence of Vcl: Forward 5' GCTTCAGTCAGACCCATACTCG 3'; reverse 5' AGGTAAGCAGTAGGTCAGATGT 3'.

REPRESENTATIVE RESULTS:

Hydrogel preparation and stiffness assessment through AFM and the Hertz model

Here, a detailed protocol is provided to generate polyacrylamide hydrogels of varying stiffness by regulating the ratio of acrylamide and bis-acrylamide. However, the polyacrylamide hydrogels are not ready for the adhesion of cells due to the lack of ECM proteins. Thus, sulfo-SANPAH, acting as a linker, covalently binds to the hydrogels and reacts with the primary amines of ECM proteins to allow the adhesion of ECM proteins to the surfaces of the hydrogels via the *N*-hydroxysuccinimide ester in sulfo-SANPAH after UV activation. Collagen type I was used as the ECM protein of choice to effectively promote O9-1 cell attachment. To ensure accurate stiffness values of different hydrogels, a stiffness assessment was performed using AFM, a well-known technique to depict the elastic modulus.

Upon successful formation and attachment of the polyacrylamide hydrogel to the glass coverslip, the gel remained adherent to the coverslip with an even surface and minimal tearing. The stiffness was measured by AFM based on the principle of indention technique, wherein a stiff indenter was applied to the sample with the required force to reach an indentation depth[26]. With

this measurement, the Young's elastic modulus was calculated based upon the indentation of depth and force in Hertz's model, an elastic theory[26]. However, due to the large variation in results by AFM, an additional statistical method was applied to obtain a quantitative result with minimal impact of uneven surfaces and imperfect homogeneity of the gel solutions[26]. To produce a quantitative measurement using AFM, a compilation of at least 50 force and distance curves from each location on the gel sample was taken for an average sample stiffness. The force applied to the high-stiffness gel was higher than that applied to the softer gel, indicating that a stiffer substrate yielded a steeper slope in the Force vs. Z graph, in which force is measured in nN, and Z indicates the indentation depth between the indenter and sample.

On soft hydrogels, the slope of the generated force curve was gentle as the required force from the AFM probe was less (**Figure 1A**). However, on stiff hydrogels, such as those with the modulus of 40 kPa, the generated slope was much steeper as the applied force was higher than for softer gels (**Figure 1B**). As the separation between the probe and the hydrogel sample decreases, the curve increases significantly as the tip of the probe touches the glass coverslip. However, as the separation distance increases, the curve merely approaches 0 as there is no applied force present.

As shown in **Figure 1A**, the cantilever on the AFM probe approached the gel, indicated by the blue line, and the probe measured the applied force required to penetrate the gel sample and eventually reach the glass coverslip, causing a sudden increase in force. Due to possible procedural and instrumental errors, such as the quality of the required solutions, the true stiffness of hydrogel samples varies largely and far from the desired stiffness. Thus, AFM is a useful tool to validate and confirm the methodology while preventing false data presentation in further experiments.

In this AFM assessment, the five prepared hydrogel samples were measured through the quantitative approach. The protocol focused on hydrogel stiffness levels of 0.5 kPa, 1 kPa, 10 kPa, 20 kPa, and 40 kPa, which mimic the breadth of biological substrate stiffness levels reported for differentiation of various cell types. The force curves obtained from AFM measurements were utilized to generate the Young's elastic modulus in kilopascals using an AFM analysis algorithm software (**Figure 2**).

Comparison of polyacrylamide hydrogel systems and cell types

This adaptation of the original protocol by Tse and colleagues provides an efficient and effective approach to study the mechanosensitive aspects of NCC using O9-1 cells[20]. Modifications to the previous protocol include modifying ECM protein incubation: replacing 50 mM HEPES with 0.2% acetic acid and the addition of 10% horse serum and FBS for cell culture (step 1.3.14–1.3.15). These modifications were validated by comparing the growth and maintenance of O9-1 NCCs on this modified gel system with that in the original (control) protocol. Here, we cultured wild-type O9-1 cells on both hydrogel systems with the elastic modulus of 1 kPa and 40 kPa for each system in basal medium. The overall cell growth status and development were visualized using a brightfield light microscope for apoptotic characteristics, stressed morphology, and cell attachment to the hydrogels. O9-1 cells grown on the original gel system resulted in a higher

number of dead cells indicated by an excess of round cells (**Figure 3E,F**) for both 1 kPa and 40 kPa hydrogels.

In contrast, the O9-1 cells grown on the modified gel system exhibited healthy cell growth and sufficient attachment to the hydrogel substrate (**Figure 3G,H**). In addition, the compatibility of NCCs with the modified hydrogel system was assessed by performing immunofluorescent staining of the NCC marker, Tcfap2α (AP-2). AP-2 is a transcription factor expressed in the NC lineages to regulate development in mouse embryos, thus making it suitable to assess compatibility[27]. Although O9-1 cells grown on control and modified hydrogel systems both expressed AP-2, there was a significant increase in AP-2 expression in O9-1 cells plated on the modified hydrogel system, as indicated by the stronger fluorescence signal and the corresponding quantification (**Figure 4A,B**).

In addition, P19 cells were used to further validate the benefits of the modified hydrogel system for the growth of cells. P19 is an embryonic carcinoma cell line that was derived from embryo-derived teratocarcinoma in mouse[28]. Using the corresponding culture protocol, P19 cells were grown on both control and modified hydrogel systems to monitor survival and growth characteristics. Brightfield imaging revealed that P19 cells plated on both hydrogel systems displayed an excess of round floating cells and a lack of cell-substrate attachments (**Figure 3A–D**). This observation suggested that the modified protocol was more suitable for O9-1 NCCs to study mechanical signaling in NCCs.

Visualization of high-stress fiber expression on stiff substrates

The modified hydrogel allowed for quantitative and qualitative analysis of the differences in the morphology of cells cultured on gels of different stiffness levels and other effectors. Once the hydrogels were ready for cell seeding, wild-type O9-1 cells were passaged onto hydrogels of different stiffness levels. Cells were monitored for their health and growth by observing their shape, spatial spread, and even attachment on the hydrogel with minimal dead cells. Some studies have shown an increase in stress fibers and cell adhesion for MSCs on high-stiffness substrates, suggesting that NCCs grown on a stiffer substrate would also exhibit similar findings compared to NCCs grown on softer substrates[29,30].

Filamentous actin (F-actin) along with myosin II, α-actinin, and other cytoskeletal proteins are known collectively as stress fibers[31]. Previous studies observed an increase in stress fiber assembly in response to increased mechanical force[31]. At one or both ends of the stress fibers, attachments to the focal adhesion complex enable cells to migrate and adhere to the ECM[31]. Phalloidin staining to visualize F-actin expression and organization in the NCCs demonstrated healthy cell growth in response to mechanical signaling (**Figure 5**). Additionally, the O9-1 cells grown on low- or high-stiffness hydrogels exhibited different morphologies through varying amounts of stress fibers (**Figure 5**). Similar to observations from reported studies performed using MSCs, it was observed that O9-1 cells grown on a stiffer substrate, 40 kPa, exhibited more stress fibers and were well-spread compared to cells grown on a softer hydrogel, indicated by 1 kPa stiffness[29,30].

Assessment of cell adhesions

To further confirm the hypothesis that the change in substrate stiffness impacts NCC adhesion, changes in *Vcl* expression were quantitatively measured via RT-qPCR in NCCs responding to different hydrogel stiffness levels. Vcl is one of the numerous cytoskeletal proteins present in the focal adhesion complex during the process of the cell establishing contacts with the substrate and sensing the ECM properties[32]. Focal adhesions are the contact points of the cells to the ECM via integrin receptors, which anchor to the cytoplasmic actin cytoskeleton, F-actin[33] The *Vcl* gene expression level suggests the changes in focal adhesions and cell adhesions of the O9-1 cells in response to the substrate stiffness.

Previous studies showed the effect of Vcl on cell adhesion in embryonic stem and fibroblast cells by differences in its expression. In response to the high expression of *Vcl*, the number and sizes of focal adhesions also increased but decreased when *Vcl* was knocked down[34]. Consistently, *Vcl*-deficient cells also showed a significant decrease in cell adhesion and spreading[35]. In addition, Vcl plays a role in regulating cell adhesion by stabilizing focal adhesions[36]. The size of focal adhesions, maturation level, and compositions vary according to the substrate stiffness, thus allowing signals to be transduced intracellularly and the cells to respond to their environmental cues[37]. Thus, Vcl is highly recruited to the focal adhesion complexes in cells grown on stiff substrates, as reflected by higher mRNA levels detected by RT-qPCR (**Figure 6C**)**.**

Cells grown on softer substrates form minimal focal adhesion complexes, as reflected by lower mRNA levels of *Vcl* in the cells[15]. In **Figure 6C**, O9-1 cells exhibited a higher expression of *Vcl* on the stiff substrate than on the soft substrate. These results suggest a higher level of cell-substrate adhesions of O9-1 cells on stiff substrates than O9-1 cells on softer substrates. In addition, Vcl expression was qualitatively visualized through IF staining with an anti-Vcl antibody to further complement and support the RT-qPCR finding. Consistently, the Vcl expression in O9-1 cells grown on the stiffer substrate was higher than those grown on the softer substrate (**Figure 6A,B**), which further supported the initial finding of high cell adhesion and spreading on the 40 kPa hydrogel in comparison to the 1 kPa hydrogel observed with F-actin phalloidin staining and *Vcl* expression levels via RT-qPCR.

FIGURE AND TABLE LEGENDS:

Figure 1: Force curves generated from the indentation of the AFM probe. F (y-axis) indicates the required force applied in nN, and Z (x-axis) indicates the Bruker AFM probe distance from the sample in µm. For the 1 kPa hydrogel (**A**), the generated slope is gentle vs. the steeper slope observed for the 40 kPa hydrogel (**B**). The colored curves represent the movement of the cantilever on the AFM probe as it approaches (blue) and retracts (red) from the hydrogel sample. The highest starting point of the curve indicates the rigid contact of the glass coverslip. (**B**) The large dip in the retracted curve in the 40 kPa hydrogel indicates adhesion between the bead and the sample. Abbreviation: AFM = atomic force microscopy.

Figure 2: The average stiffness of hydrogels (in kPa) calculated from the Young's elastic modulus. The Young's modulus was generated from the force curves from **Figure 1.** The

referenced elastic moduli of the hydrogels were 0.5 kPa, 1 kPa, 10 kPa, 20 kPa, and 40 kPa. Error bars indicate standard deviation.

Figure 3: Bright-field images of P19 and O9-1 cells plated on 1 kPa and 40 kPa hydrogels of control and modified gel systems to detect cell growth characteristics. (**A–D**) P19 and (**E–H**) O9-1 cells; dead cells are indicated by red arrows. Scale bars = 25 µm.

Figure 4: Immunofluorescence staining of NCC marker AP-2 in O9-1 NCCs to visualize NCC compatibility. (**A**) A 40 kPa modified hydrogel system compared to (**B**) a 40 kPa control. AP-2 (green); nuclei were stained with DAPI (blue). Scale bars = 25 µm. (**C**) Bar graph provides quantification of the AP-2 expression level showing significance (*p*-value = 0.003) (n = 3). Data show the relative expression with provided standard deviation error bars. Abbreviations: NCC = neural crest cell; DAPI = 4′,6-diamidino-2-phenylindole.

Figure 5: Fluorescent phalloidin staining of F-actin showing stress fibers that are well-spread out in O9-1 cells on the 40 kPa hydrogel. O9-1 cells were cultured on 1 kPa (**A**) and 40 kPa hydrogels (**B**). O9-1 cells were stained using Alexa Fluor 488 Phalloidin (green), and the nuclei were stained with DAPI (blue). Scale bars = 25 µm. Abbreviation: DAPI = 4′,6-diamidino-2-phenylindole.

Figure 6: **Immunofluorescence images of vinculin in O9-1 cells**. O9-1 cells were plated on 1 kPa (**A**) and 40 kPa (**B**) hydrogels. Nuclei were stained with DAPI (blue). Scale bars = 25 µm. (**C**) Real-time quantitative PCR analysis of the total mRNA level of *Vcl* in O9-1 cells cultured on 1 kPa and 40 kPa hydrogels. Vcl expression level on the 1 kPa hydrogel is significantly lower than that on the 40 kPa hydrogel (*p*-value = 0.02). Data shows the average with provided standard deviation error bars. Abbreviation: DAPI = 4′,6-diamidino-2-phenylindole.

Table 1: Corresponding volumes of solutions to obtain the desired stiffness levels.

DISCUSSION:

In the current study, the goal was to provide an effective and efficient *in vitro* system to better understand the impact of mechanical signals in NCCs. In addition to following the step-by-step protocol mentioned above, researchers need to keep in mind that the cell culture of O9-1 NCCs is affected by the type of glass coverslips used to prepare hydrogels. For instance, it was noted that cells seeded on a specific type of glass coverslip (see the **Table of Materials**) survived and proliferated well, while cultured cells seeded on other types of glass coverslips showed more cell death. Furthermore, it is important to strictly follow the correct cell culture conditions for O9-1 NCCs[38]. The quality of the cell culture is optimal when the hydrogels are used as soon as possible or stored in a sterile 37 °C incubator for up to two days.

Due to the sensitivity of each component in the protocol, the elastic moduli could vary across experiments. In addition to the points mentioned in the protocol (step 1.3.2) regarding 10% APS, other critical factors to keep in mind also affect the variation. Another factor that was suspected of causing large variations in AFM measurements was the thickness of the hydrogels. A previous

study had investigated the effect of thickness on the Young's moduli, ranging from 15 to 1000 µm, and had found that differences in thickness did not change the Young's moduli significantly[39]. However, the thickness of the substrates also affects the mechanical properties that the cells can sense, leading to different morphologies[40,41,42]. Various studies showed that a significant increase in the thickness of hydrogels led to a decrease in the cell area, spreading, and effective stiffness of hydrogels[40,41,42]. However, the phenotypes of cells also change in response to significantly thin hydrogels, e.g., higher spreading even on low-stiffness hydrogels[40,41,42]. With a consistent volume of polyacrylamide gels, the thickness of hydrogels should be uniform so that slight deviations will not significantly affect the elastic modulus in AFM measurements.

It is better to sterilize coverslips by passing them back and forth in the flame using an alcohol burner because other sterilization methods can be more complicated and cause potential damage to the glass coverslips. Different sizes of glass coverslips can be used based on experimental requirements. This protocol utilized 12 mm and 25 mm coverslips for immunohistochemistry and RT-qPCR, respectively. Using appropriately sized gels to suit the experiments encourages efficiency and minimizes waste. These modifications were validated qualitatively and quantitatively to ensure optimization for O9-1 NCCs compared to the original (control) hydrogel system[20]. The overall health and growth of O9-1 NCCs were assessed under a brightfield microscope for cellular and substrate attachment characteristics.

In addition, the compatibility of O9-1 cells was compared between both control and the modified hydrogel systems to further validate the modifications in this protocol by qualitatively visualizing AP-2 expression using IF staining. The intensity of the signals was quantified to further support the representative images of AP-2 expression in O9-1 cells between control vs. the modified hydrogel systems. While AP-2 is a common NCC marker, other well-known markers must be considered for validation, such as Sox10 and Pax3, due to their significance for NCC maintenance of pluripotency and survival[28]. In addition, the optimization in this protocol was further confirmed by comparing the O9-1 NC cells with another cell line, P19, to ensure that this hydrogel system is efficient and reliable for NC cells. Although P19 cells have immortal characteristics and are easily cultured, they did not thrive well on either of the hydrogel systems.

The resistance to the elongating force generated from the substrate or tissue stiffness where the cells attach is often expressed as Young's elastic modulus[45]. With AFM, the Young's elastic modulus is obtained from the force curve generated from the applied vertical force[26]. Large variations can occur during AFM measurement, between measurements that can lead to inaccurate readings for the stiffer hydrogels. The inconsistency can be caused by improper probes used for measurement. For instance, measurement of 20 kPa and 40 kPa hydrogels require the use of a stiffer probe with a higher spring constant (k = 0.24 N/m). A stiffer probe allows for a lower resolution compared to a softer probe; however, there are reasons to favor the choice of a stiffer probe as too-soft cantilevers could adhere to the samples[46]. In addition, too-soft probes are highly sensitive, contributing to false signals from unwanted particles and resulting in artificially lower or higher stiffness values than the true stiffness[46]. Furthermore, accurate input of Poisson's ratio must be noted, depending on the measuring material; this could be found in standardized studies as this significantly affects the data output.

In addition, AFM was utilized to measure the thickness of the hydrogels, as thickness is another mechanical property affecting how cells sense their environment[47,42]. In various reported studies, cells that are grown on soft hydrogels are observed to be round in shape at and beyond "critical thickness," which is reported at ~2–5 μm, depending on the cell type[47,42,48]. However, much higher spreading was observed when cells were plated on hydrogels of the same stiffness but lower thickness than the "critical thickness"[42,48]. A potential explanation for this interesting finding is that the sub-critical thickness of hydrogels enables the cells to sense the rigid underlying glass coverslips as the cells exert traction for lateral displacement[47]. The average thickness across all-stiffness hydrogels was 342 μm with a standard deviation of 27 μm. The thickness of the hydrogels was higher than the suggested "critical thickness", and within the testing range of under 400 μm, which was reported in studies and the manufactured premade hydrogels, such that the cells could sense the different stiffness of the hydrogels and not the underlying rigid glass coverslips[42,48].

In addition to the AFM quantitative analysis method, the hydrogels were also qualitatively analyzed through immunohistochemistry to study the expression of the markers affected by the varying stiffness in O9-1 cells and to visualize healthy growth of the cells. F-actin in the cytoplasm is connected to the membrane-bound integrins via a set of cytoskeletal proteins, such as talin and Vcl, forming the focal adhesion complex[33]. Expression of stress fibers in cells could also be analyzed by measuring the expression of other cytoskeletal genes in cells, such as talin and integrin, which could be visualized together using the focal adhesion staining kit.

There were varying degrees of hydrogel stiffness that influenced NCC morphology and response, as seen in the change in cell adhesion and stress fibers through mechanical signaling. This protocol offers the ability to influence cell differentiation into various cell types by modifying the corresponding culture conditions *in vitro*, thus providing a convenient method of manipulation of mechanical signals and chemical signals in NCCs. As mentioned previously, the fate of NCC differentiation is largely guided by mechanical forces present in the surrounding tissue, including its stiffness[2,3]. While the immediate goal of this paper was to develop a step-by-step protocol to prepare hydrogels for NCC culture, the potential benefits of this protocol extend beyond the methodology, pursuing further knowledge of mechanical signaling in NCCs. It is also worth noting that this *in vitro* system has some limitations. This technique of fabricating hydrogels comprises multiple steps that can potentially introduce technical variations along the way, including heterogeneity, uneven surface, and inaccurate stiffness. Therefore, users must perform these steps carefully to minimize technical variations during experiments. In addition, polyacrylamide gels in this system limited studies to 2D culture due to the toxicity of acrylamide, ignoring the precise 3D biological environment that NCCs inhabit[50].

Despite these constraints, this *in vitro* system allows for an inexpensive and simple method benefiting all levels of research and enabling researchers to perform sufficient and functional downstream tests. As seen in recent findings, NCCs rely heavily on both mechanical signaling, such as shear force and substrate stiffness, and chemical signaling, such as Wnt and fibroblast growth factor signaling, in craniofacial, as well as heart development in vertebrates[6,15]. Using this

protocol, the local microenvironments for *in vitro* experiments can be easily mimicked for future studies on NCCs, including differentiation, migration, cellular responses, and the potential of detrimental disease progression. Therefore, this *in vitro* system will be a powerful tool to study the roles of mechanical signaling in NCCs and their interactions with other signaling pathways, which will deepen the understanding of the molecular and genetic mechanisms of NCC development and related diseases.

ACKNOWLEDGMENTS:

We thank Dr. Ana-Maria Zaske, operator of Atomic Force Microscope–UT Core facility at the University of Texas Health Sciences Center, for the contributed expertise in AFM in this project. We also thank the funding sources from the National Institutes of Health (K01DE026561, R03DE025873, R01DE029014, R56HL142704, and R01HL142704 to J. Wang).

DISCLOSURES:

The authors have no conflicts of interest to disclose.

REFERENCES:

1. Mehrotra, P., Tseropoulos, G., Bronner, M. E. Andreadis, S. T. Adult tissue-derived neural crest-like stem cells: Sources, regulatory networks, and translational potential. *Stem Cells Translational Medicine*. **9** (3), 328–341 (2020).
2. Liu, J. A., Cheung, M. Neural crest stem cells and their potential therapeutic applications. *Developmental Biology.* **419** (2), 199–216 (2016).
3. Watt, K. E. N., Trainor, P. A. Neurocristopathies: the etiology and pathogenesis of disorders arising from defects in neural crest cell development. In *Neural Crest Cells—Evolution, Development and Disease*, Trainor, P. A. (Ed), Academic Press, 361–394 (2014).
4. Lavelle, C. L. B. Applied oral physiology. Butterworth-Heinemann (1988).
5. Chin, L. The genetics of malignant melanoma: lessons from mouse and man. *Nature Reviews Cancer.* **3** (8), 559–570 (2003).
6. Hindley, C. J. et al. The Hippo pathway member YAP enhances human neural crest cell fate and migration. *Scientific Reports.* **6** (1), 1–9 (2016).
7. Wang, Q. et al. Perturbed development of cranial neural crest cells in association with reduced sonic hedgehog signaling underlies the pathogenesis of retinoic-acid-induced cleft palate. *Disease Models & Mechanisms.* **12** (10), dmm040279 (2019).
8. Rocha, M., Singh, N., Ahsan, K., Beiriger, A., Prince, V. E. Neural crest development: insights from the zebrafish. *Developmental Dynamics.* **249** (1), 88–111 (2020).
9. Barriga, E. H., Franze, K., Charras, G., Mayor, R. Tissue stiffening coordinates morphogenesis by triggering collective cell migration in vivo. *Nature.* **554** (7693), 523–527 (2018).
10. Weber, G. F., Bjerke, M. A., DeSimone, D. W. A mechanoresponsive cadherin-keratin complex directs polarized protrusive behavior and collective cell migration. *Developmental Cell.* **22** (1), 104–115 (2012).
11. Mason, D. E. et al. YAP and TAZ limit cytoskeletal and focal adhesion maturation to enable persistent cell motility. *Journal of Cell Biology.* **218** (4), 1369–1389 (2019).
12. Dupont, S. et al. Role of YAP/TAZ in mechanotransduction. *Nature.* **474** (7350), 179–183 (2011).

13. Lu, Y. -B. et al. Viscoelastic properties of individual glial cells and neurons in the CNS. *Proceedings of the National Academy of Sciences of the United States of America.* **103** (47), 17759–17764 (2006).
14. Georges, P. C., Miller, W. J., Meaney, D. F., Sawyer, E. S., Janmey, P. A. Matrices with compliance comparable to that of brain tissue select neuronal over glial growth in mixed cortical cultures. *Biophysical Journal.* **90** (8), 3012–3018 (2006).
15. Janmey, P. A., Miller, R. T. Mechanisms of mechanical signaling in development and disease. *Journal of Cell Science.* **124** (1), 9–18 (2011).
16. Engler, A., Sweeney, H., Discher, D., Schwarzbauer, J. E. Extracellular matrix elasticity directs stem cell differentiation. *Journal of Musculoskeletal and Neuronal Interactions.* **7** (4), 335 (2007).
17. Paszek, M. J. et al. Tensional homeostasis and the malignant phenotype. *Cancer Cell.* **8** (3), 241–254 (2005).
18. Engler, A. J. et al. Embryonic cardiomyocytes beat best on a matrix with heart-like elasticity: scar-like rigidity inhibits beating. *Journal of Cell Science.* **121** (22), 3794–3802 (2008).
19. Robling, A. G., Turner, C. H. Mechanical signaling for bone modeling and remodeling. *Critical Reviews in Eukaryotic Gene Expression.* **19** (4), 319–338 (2009).
20. Tse, J. R., Engler, A. J. Preparation of hydrogel substrates with tunable mechanical properties. *Current Protocols in Cell Biology.* Chapter 10, Unit 10.16 (2010).
21. Cretu, A., Castagnino, P., Assoian, R. Studying the effects of matrix stiffness on cellular function using acrylamide-based hydrogels. *Journal of Visualized Experiments: JoVE.* (42), 2089 (2010).
22. Ishii, M. et al. A stable cranial neural crest cell line from mouse. *Stem Cells and Development.* **21** (17), 3069–3080 (2012).
23. Engler, A. et al. Substrate compliance versus ligand density in cell on gel responses. *Biophysical Journal.* **86** (1), 617–628 (2004).
24 Stanton, A. E., Tong, X., Yang, F. Varying solvent type modulates collagen coating and stem cell mechanotransduction on hydrogel substrates. *APL Bioengineering.* **3** (3), 036108 (2019).
25. Fedoroff, S., Hall, C. Effect of horse serum on neural cell differentiation in tissue culture. *In vitro.* **15** (8), 641–648 (1979).
26. Huth, S., Sindt, S., Selhuber-Unkel, C. Automated analysis of soft hydrogel microindentation: Impact of various indentation parameters on the measurement of Young's modulus. *PLoS One.* **14** (8), e0220281 (2019).
27. Mitchell, P. J., Timmons, P. M., Hébert, J. M., Rigby, P., Tjian, R. Transcription factor AP-2 is expressed in neural crest cell lineages during mouse embryogenesis. *Genes & Development.* **5** (1), 105–119 (1991).
28. Wegner, M. Neural crest diversification and specification: transcriptional control of Schwann Cell differentiation. Encyclopedia of Neuroscience. 153–158 (2010).
29. Park, J. S. et al. The effect of matrix stiffness on the differentiation of mesenchymal stem cells in response to TGF-β. *Biomaterials.* **32** (16), 3921–3930 (2011).
30. Sun, M. et al. Effects of matrix stiffness on the morphology, adhesion, proliferation and osteogenic differentiation of mesenchymal stem cells. *International Journal of Medical Sciences.* **15** (3), 257 (2018).

31. Burridge, K., Guilluy, C. Focal adhesions, stress fibers and mechanical tension. *Experimental Cell Research.* **343** (1), 14–20 (2016).
32. Burridge, K. Focal adhesions: a personal perspective on a half century of progress. *The FEBS Journal.* **284** (20), 3355–3361 (2017).
33. Zhou, C. *et al.* Compliant substratum modulates vinculin expression in focal adhesion plaques in skeletal cells. *International Journal of Oral Science.* **11 (2)**, 1–9 (2019).
34. Fernández, J. L. R., Geiger, B., Salomon, D., Ben-Ze'ev, A. Overexpression of vinculin suppresses cell motility in BALB/c 3T3 cells. *Cell Motility and the Cytoskeleton.* **22** (2), 127–134 (1992).
35. Coll, J. et al. Targeted disruption of vinculin genes in F9 and embryonic stem cells changes cell morphology, adhesion, and locomotion. *Proceedings of the National Academy of Sciences of the United States of America.* **92** (20), 9161–9165 (1995).
36. Saunders, R. M. et al. Role of vinculin in regulating focal adhesion turnover. *European Journal of Cell Biology.* **85** (6), 487–500 (2006).
37. Kuo, J. -C. Focal adhesions function as a mechanosensor. *Progress in Molecular Biology and Translational Science.* **126**, 55–73 (2014).
38. Nguyen, B. H., Ishii, M., Maxson, R. E., Wang, J. Culturing and manipulation of O9-1 neural crest cells. *Journal of Visualized Experiments: JoVE.* (140), 58346 (2018).
39. Kolewe, K. W., Zhu, J., Mako, N. R., Nonnenmann, S. S., Schiffman, J. D. Bacterial adhesion is affected by the thickness and stiffness of poly (ethylene glycol) hydrogels. *ACS Applied Materials & Interfaces.* **10** (3), 2275–2281 (2018).
40. Lin, Y. -C. et al. Mechanosensing of substrate thickness. *Physical Review E.* **82** (4), 041918 (2010).
41. Mullen, C. A., Vaughan, T. J., Billiar, K. L., McNamara, L. M. The effect of substrate stiffness, thickness, and cross-linking density on osteogenic cell behavior. *Biophysical Journal.* **108** (7), 1604–1612 (2015).
42. Tusan, C. G. et al. Collective cell behavior in mechanosensing of substrate thickness. *Biophysical Journal.* **114** (11), 2743–2755 (2018).
43. McBurney, M. W., Jones-Villeneuve, E. M., Edwards, M. K., Anderson, P. J. Control of muscle and neuronal differentiation in a cultured embryonal carcinoma cell line. *Nature.* **299** (5879), 165–167 (1982).
44. Hasegawa, A.; Shirayoshi, Y., P19 cells overexpressing Lhx1 differentiate into the definitive endoderm by recapitulating an embryonic developmental pathway. *Yonago Acta Medica.* **58** (1), 15 (2015).
45. Wells, R. G. Tissue mechanics and fibrosis. *Biochimica et Biophysica Acta.* **1832** (7), 884–890 (2013).
46. Gavara, N. A beginner's guide to atomic force microscopy probing for cell mechanics. *Microscopy Research and Technique.* **80** (1), 75–84 (2017).
47. Butler, J. P., Tolic-Nørrelykke, I. M., Fabry, B., Fredberg, J. J. Traction fields, moments, and strain energy that cells exert on their surroundings. *American Journal of Physiology. Cell Physiology.* **282** (3), C595–C605 (2002).
48. Leong, W. S. et al. Thickness sensing of hMSCs on collagen gel directs stem cell fate. *Biochemical and Biophysical Research Communications.* **401** (2), 287–292 (2010).

49. Caliari, S. R., Burdick, J. A. A practical guide to hydrogels for cell culture. *Nature Methods.* **13** (5), 405–414 (2016).
50. Funaki, M., Janmey, P. A. Technologies to engineer cell substrate mechanics in hydrogels. *Biology and Engineering of Stem Cell Niches.* Academic Press, 363–373 (2017).

Figure 1 (combined A and B)

Click here to access/download;Figure;Fig1 7-8-21.tiff

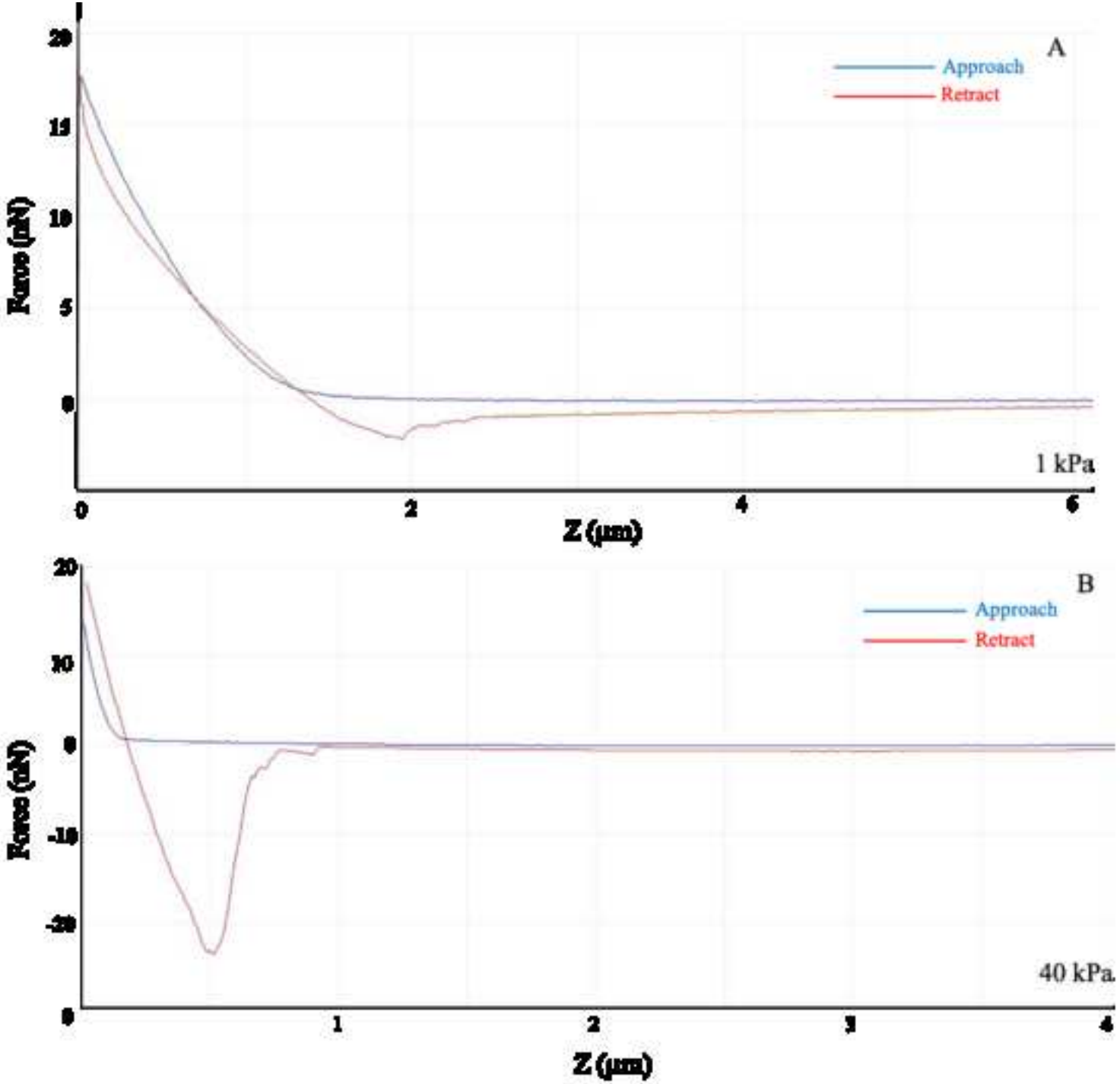

Figure

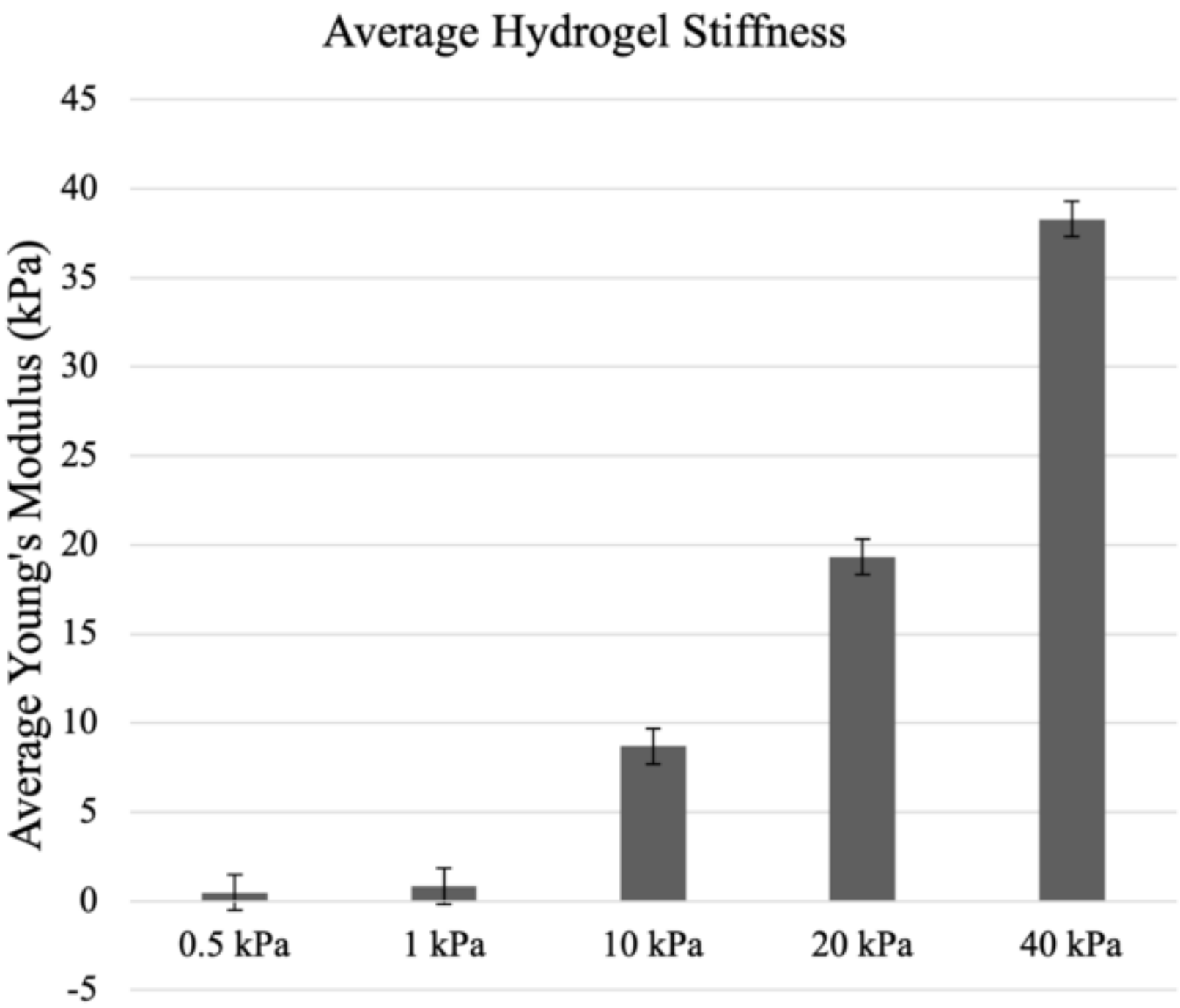

Figure

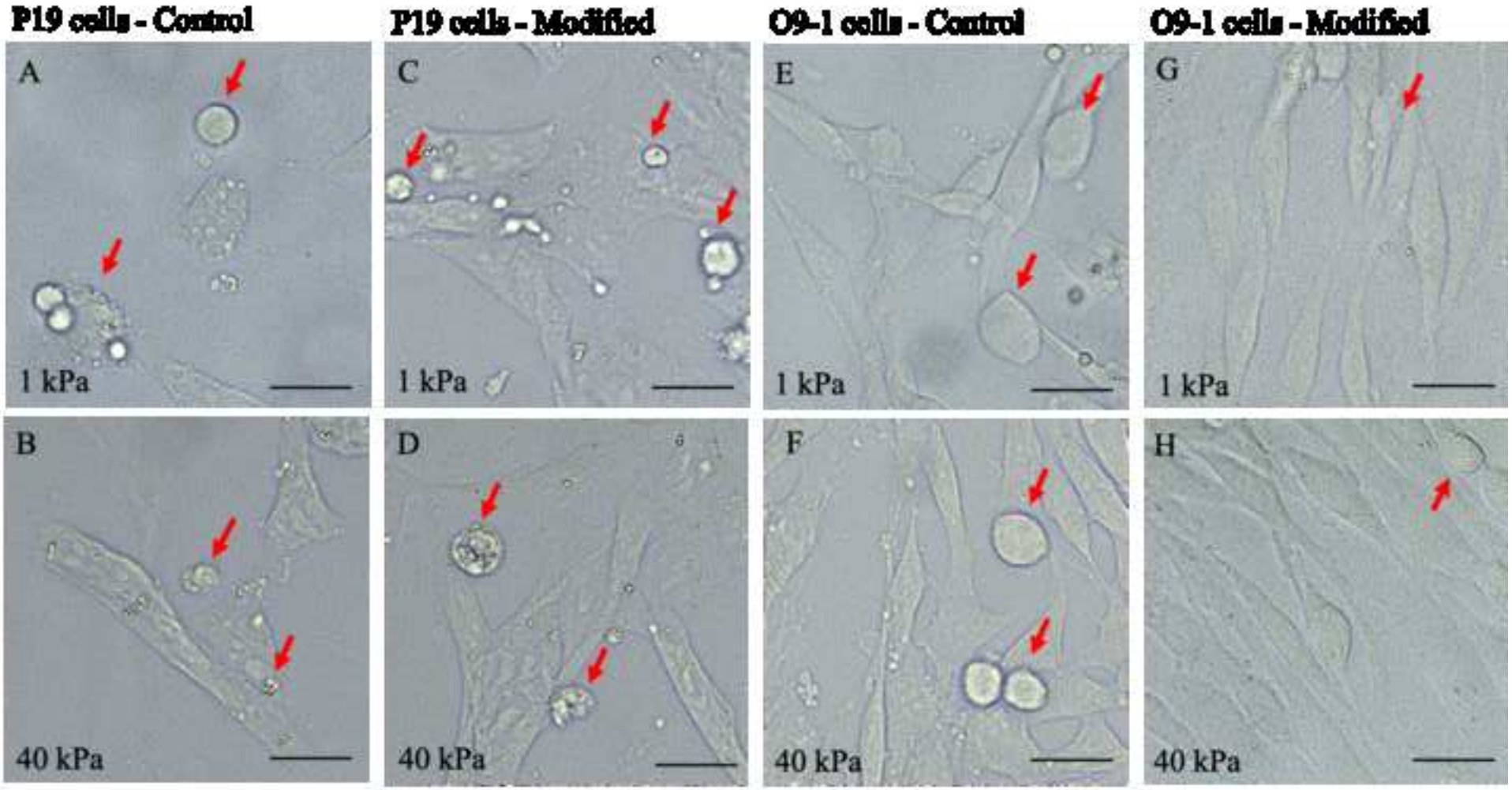

Figure

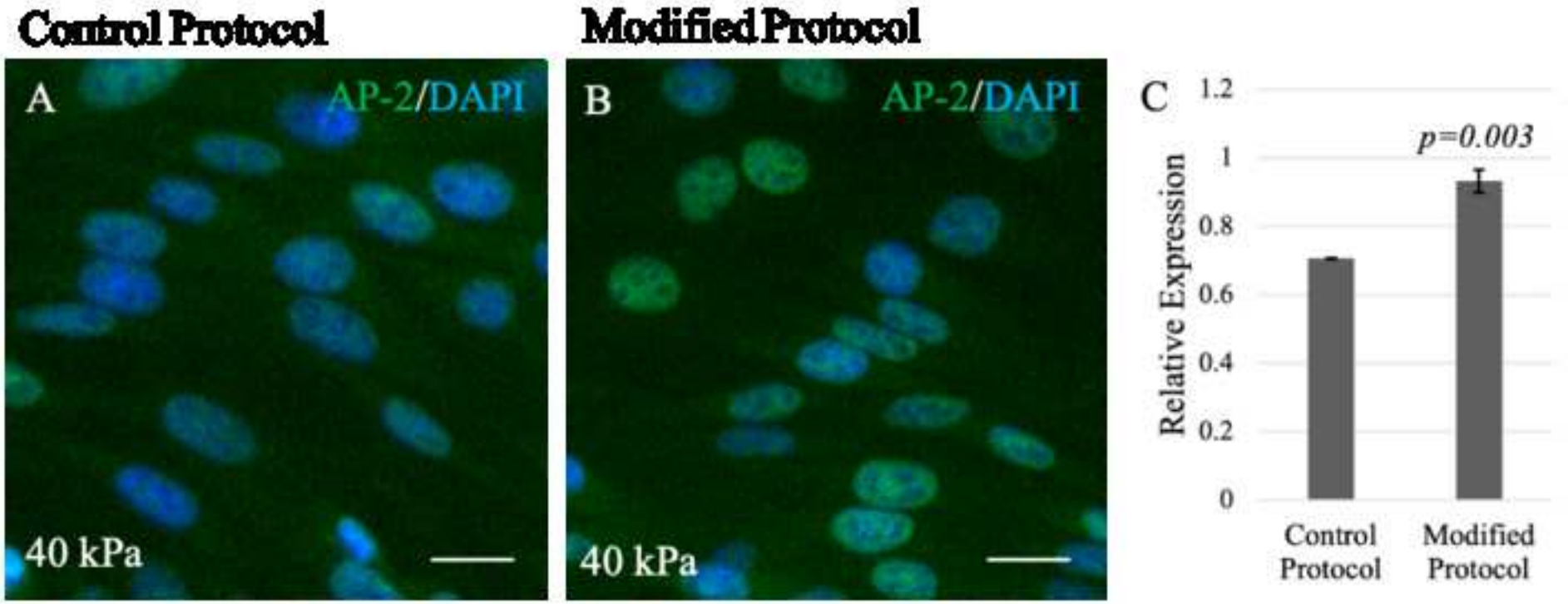

Figure

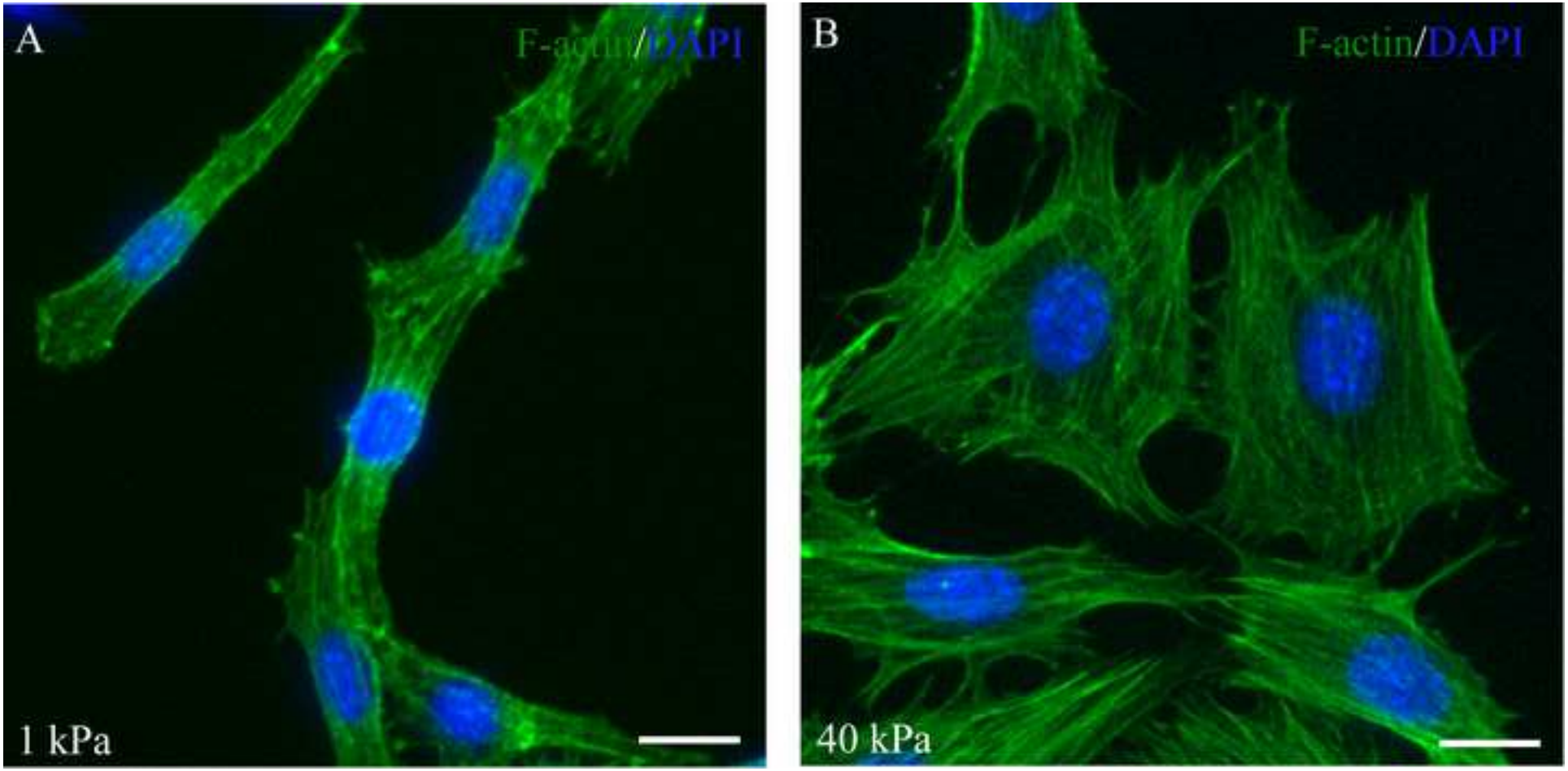

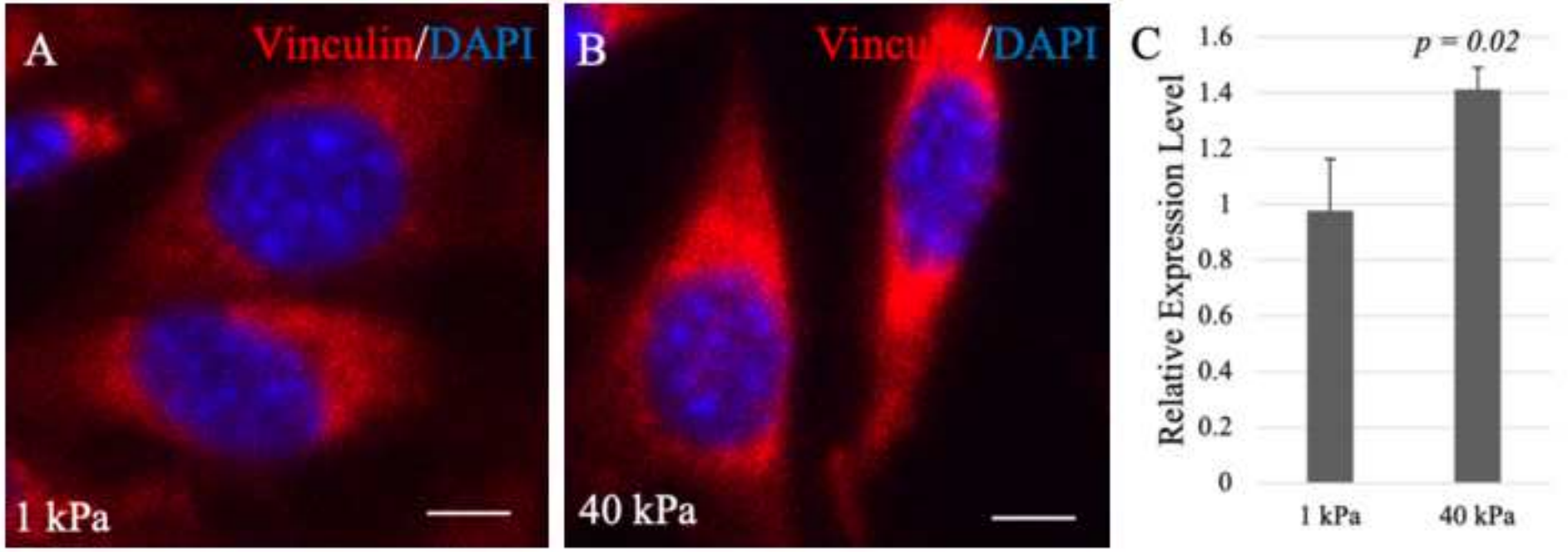

Table 1 Click here to access/download;Table;Table 1 (17).xlsx

500 μL total volume	0.5 kPa	1 kPa	10 kPa	20 kPa	40 kPa
40% Acrylamide (μL)	37.5	62.5	125	100	100
20% Bis-acrylamide (μL)	15	7.5	25	66	120
H_2O (μL)	447.5	430	350	334	280
10% APS (μL)	5	5	5	5	5
TEMED (μL)	0.5	0.5	0.5	0.5	0.5

Jun 21, 2021
Vidhya Iyer, Ph.D.
Review Editor, JoVE

RE: “An efficient in vitro system to study mechanical signals in neural crest cells” (JoVE62693)

Dear Dr. Iyer,

We thank you and both reviewers for evaluating our manuscript and providing valuable feedback about our work. We are now resubmitting the revised manuscript after having performed extensive additional experiments. Below you will find our point-by-point response to the editor and reviewers’ comments.

Editor’s Comments:

Based on your comments regarding the necessary technical issues including grammatical errors, spellings, etc., we addressed and made changes accordingly to the concerns below.

1. “Please take this opportunity to thoroughly proofread the manuscript to ensure that there are no spelling or grammar issues. Please define all abbreviations at first use.”

   The manuscript was carefully proofread and revised several times by all authors to address any spelling and grammatical errors presented in the manuscript. Moreover, we defined all abbreviations at first use including neural crest (NC), mesenchymal stem cells (MSCs), and chemical names.

2. “Please provide an email address for each author.”

   As suggested, email address for each author was provided beside their names in the author section.

3. “Please revise the following lines to avoid overlap with previously published work: 74-76.”

   As suggested, we revised lines 74-76 in order to avoid the overlapping of words use with previous published work.

4. “Please remove the embedded Table from the manuscript. All tables should be uploaded separately to your Editorial Manager account in the form of an .xls or .xlsx file. The table legend or caption (title and description) should appear in the Figure and Table Legends section after the Representative Results in the manuscript text.”

   Table 1 has been removed from the manuscript document and will be submitted separately as an .xls file. In addition, we also moved the caption of table 1 to the Figure and Table legend portion.

5. “Please revise the text, especially in the protocol, to avoid the use of any personal pronouns (e.g., "we", "you", "our" etc.)”

   We removed all personal pronouns as much as possible in the main text, specifically in the protocol.

6. “Please ensure that all text in the protocol section is written in the imperative tense as if telling someone how to do the technique (e.g., “Do this,” “Ensure that,” etc.). The actions should be described in the imperative tense in complete sentences wherever possible. Avoid usage of phrases such as “could be,” “should be,” and “would be” throughout the Protocol. Any text that cannot be written in the imperative tense may be added as a “Note.” However, notes should be concise and used sparingly. Please include all safety procedures and use of hoods, etc.”

   We revised all protocol steps to be in imperative tense, and removed all “should be”, “would be”, etc. Moreover, we also removed some of the unnecessary “Note:” as suggested and supplemented those in the discussion section. We additionally stated in the beginning of the protocol and discussion section that all the steps of making the hydrogels are performed in a hood to avoid overcrowding the protocol section.

7. “JoVE cannot publish manuscripts containing commercial language. This includes trademark symbols (™), registered symbols (®), and company names before an instrument or reagent. Please remove all commercial language from your manuscript and use generic terms instead. All commercial products should be sufficiently referenced in the Table of Materials and Reagents.”

   As noted, we removed all commercialized brand names of instruments and reagents used in the manuscript and replaced them with generic names. Name brands are mentioned in the material table.

8. “Please note that your protocol will be used to generate the script for the video and must contain everything that you would like shown in the video. Please ensure you answer the “how” question, i.e., how is the step performed? Alternatively, add references to published material specifying how to perform the protocol action. Please ensure specific details (*e.g.* button clicks for software actions, numerical values for settings, etc) are present in your protocol steps. There should be enough detail in each step to supplement the actions seen in the video so that viewers can easily replicate the protocol.”

   As suggested, we supplemented details to the manuscript protocol that will be used for the video script (*i.e.* hydrogel protocol). I also highlighted the portion that will be used as the video script. I hope that this is sufficient for the video script.

9. “The Protocol should be made up almost entirely of discrete steps without large paragraphs of text between sections. Please simplify the Protocol so that individual steps contain only 2-3 actions per step and a maximum of 4 sentences per step. In the JoVE Protocol format, “Notes” should be concise and used sparingly. They should only be used to provide extraneous details, optional steps, or recommendations that are not critical to a step. Please consider moving some of the notes about the protocol to the discussion section.”

   Each step in the protocol was simplified and broken up into concise and direct steps. We also moved some of the “Note” into the discussion section such as “The quality of cell culture is the healthiest and best when the hydrogels are used as soon as possible or stored in the sterile 37^{o}C incubator up to two days.” which is in the 1.3.20 step.

10. “Please format the manuscript as: paragraph Indentation: 0 for both left and right and special: none, Line spacings: single. Please include a single line space between each step, sub-step and note in the protocol section. Please use Calibri 12 points and one-inch margins on all the side. After including a one-line space between each protocol step, highlight up to 3 pages of protocol text for inclusion in the protocol section of the video. This will clarify what needs to be filmed.”

    We reformatted the manuscript following the guideline including indentation, spacing, margin, font and font size. We also highlighted the portion of the protocol that will be used for the video script.

11. “Please add limitations of your technique and the significance with respect to existing methods to your discussion.”

    The limitations and advantages of this technique in respect to existing methods in the field were added to the discussion section, specifically line 567-575.

12. “Please include a space between numbers and units, e.g., 1 kPa (not 1KPa) in fig 4 and 5”

    In the revised version, the space is now included between number and unit in the figure legend and throughout the manuscript.

13. “Please sort the Materials Table alphabetically by the name of the material.”

    Material table in the excel file is sorted in alphabetical order by the name of the material.

Reviewer 1:

Reviewer 1 noted “The development of methods to study the role of mechanics on development and cell differentiation is an important area of research”. Moreover, this reviewer also noted some concerns as follow:

1. “This manuscript claims the optimization of such methods for the neural crest cells; however, the changes are minimal and probably optimized for the particular cell line used (O9-1 cells). For example, the authors say, "Another change is to sterilize coverslips using the method of passing it back and forth in the flame using an alcohol burner", this is a trivial modification, frequently used in many laboratories, or "One of the major changes made in this protocol is to incubate hydrogels in Collagen I at 37oC overnight", this is almost certain dependent on the cell type and cannot be described as an optimized method for 'neural crest' in general.”

    We thank the reviewer for this comment. We have revised our discussion part accordingly to focus on major modifications such as “One of the changes made in this protocol is to incubate hydrogels in Collagen I, diluted in 0.2% acetic acid instead of 50 mM HEPES at 37^{o}C overnight. The low pH of acetic acid as the solvent leads to a homogenous distribution and higher amounts of Collagen I incorporation, thus a more even attachment of the ECM protein” In addition, we showed data to compare culturing

the O9-1 cells on hydrogels made according to both the original and modified protocol, which we found the modification have benefited the cell culture.

We further supplemented additional information and discussion regarding O9-1 cells as a powerful model for studying neural crest cells in vitro. O9-1 cells are a stable NC cell line that were isolated from mouse embryo (E) at E8.5, and able to mimic NC *in vivo* by differentiating into various NC derived cell types. Therefore O9-1 cells are utilized as a nice in vitro model to study the effects and changes of NCCs in response to mechanical changes. We hope this will provide more insights about O9-1 cells for the readers and why O9-1 cell is the NCCs model for *in vitro* experiments.

2. "The author conclude that cells increase adhesion to the substrate in stiffer gels by analysing the levels of vinculin. This conclusion is incorrect, as they need to analyse focal adhesion, as vinculin levels are not a direct red-out of focal adhesions."

   We thank the reviewer for this comment. We agree that the expression of Vinculin does not directly display focal adhesions as focal adhesions are composed of other proteins as well. Yet it has been build that Vinculin could reflect the focal adhesion, so we have modified the conclusion to present our data more accurately. In many studies across various cell types, the increase of Vinculin recruitment or overexpression of vinculin are observed to have higher cell adhesion, while Vinculin knock-down led to decrease of cell adhesion and also decrease in size of focal adhesion. These indicate the connection between vinculin and focal adhesion of cells. In addition, we have showed the immunofluorescence staining of vinculin from 1 kPa and 40 kPa to compliment the RT-qPCR data in our revised manuscript.

3. "Figures 1 does not contribute to the method and could be deleted."

   As suggested, we have removed the figure 1.

Reviewer 2:

We thank the reviewer for the positive comment "Overall, the experimental design, data acquisition, analyses and interpretation are sounded and reasonably convincing. It would make significant impact on research of mechanical signaling of NCCs with the modified PA gel system."

However, reviewer 2 also raised some key concerns that could benefit and strengthen the overall manuscript. We have done more experiments and addressed these concerns below:

1. "It would be necessary to have a type of control PA gel and a type of cell other than NCC working side-by-side with this modified PA gel system and NCCs to provide comparative data in supporting the conclusions. Specifically, the gene expressions of major NCCs markers may be presented to show the compatibility of the gel systems to the NCCs. This is critical to claim the significance of having a reliable and efficient system for NCCs."

   We thank the reviewer for the suggestions and have performed further experiments as suggested. We have cultured wild type O9-1 cells onto both gel systems that made following our modified protocol and the original protocol. We found the NCC marker, Tfap2α,was expressed in O9-1 cells cultured on both system, while expression is

stronger in cells grown on the modified system compared to the original one, suggesting the modifications benefitted maintenance of NCCs.

We also supplemented another cell line, P19, and assessed its growth on the gel systems comparing to our model, O9-1 NCC. P19 is an embryonic carcinoma cell line that is derived from embryo-derived tetrocarcinoma in mice. Using their corresponding protocol for culture, both cell lines were plated onto 1 kPa and 40 kPa and the cell growth quality of each cell line was observed. The P19 cells did not grow as healthy as O9-1 cells.

2. “It is recommended to add the immunocytochemistry images of vinculin on low and high stuffiness gels to complement and further support the qPCR data.”

   We thank the reviewer for this suggestion. We have added the immunofluorescence images of Vinculin of WT O9-1 cells plated on 1 kPa and 40 kPa hydrogels to complement and further support the RT-qPCR data in the manuscript.

3. “In addition to uneven surfaces and imperfect homogeneity of the gel solutions on coverslip, please comment on the possible effect of gel thickness on the large variations of your AFM measurements. What is the average thickness of your modified PA gel of various stiffness on coverslip?”

   As suggested, we have supplemented the possible effect of gel thickness on the variations of the AFM measurement in the discussion section. We referenced a reported study that investigated the variation in thickness (from 15-1000 μm) affecting the Young’s moduli via AFM, which they concluded the differences in Young’s moduli between thickness were not significant. In addition, we also measured the thickness of the hydrogels via AFM. The average thickness of the hydrogels was measured to be approximately 342.6 μm with the standard deviation of 27μm from the center to the outer area of the gel in order to monitor the varying thickness across the surface.